TITLE:

The Effect of the Anion Fraction on the Physicochemical Properties of EMIm(HF)nF (n= 1.0–2.6)

AUTHOR(S):

Hagiwara, Rika; Nakamori, Yoji; Matsumoto, Kazuhiko; Ito, Yasuhiko

The effect of the anion fraction on the physicochemical properties of EMIm(HF)$_n$F (n = 1.0 ~ 2.6)

Rika Hagiwara, Yoji Nakamori, Kazuhiko Matsumoto, Yasuhiko Ito

Graduate School of Energy Science, Kyoto University, Sakyo-ku, Kyoto 606-8501, Japan

E-mail: hagiwara@energy.kyoto-u.ac.jp

Abstract

A series of molten salts EMIm(HF)$_n$Fs with different n values has been synthesized by the reaction of EMImHF$_2$ and anhydrous hydrogen fluoride. The salts contain EMIm cation and some oligomeric fluorohydrogenate anions, (HF)$_n$F$^-$, of which the fraction changes with the change of n. A phase diagram of EMIm(HF)$_n$Fs (n =1.0~2.6) has been constructed which suggests the presence of the stoichiometric compounds, EMIm(HF)$_{1.5}$F and EMIm(HF)$_2$F in this range. Compared to EMIm(HF)$_{2.3}$F previously reported, EMIm(HF)$_n$Fs (n =1.8~2.0) possess wider liquid temperature ranges because of their similar melting points and superior thermal stabilities at elevated temperatures. The electrochemical windows of EMIm(HF)$_n$Fs (n =1.0~2.6) falls in the range of 2.9 to 3.4 V. The conductivity of EMIm(HF)$_n$Fs (n =1.0~2.6) increases with the increase of n.

Keywords

molten salt, ionic liquid, imidazolium, fluoride, fluorohydrogenate

Briefs

A series of molten salts $EMIm(HF)_nFs$ with different n values has been synthesized by the reaction of $EMImHF_2$ and anhydrous hydrogen fluoride. Their physicochemical properties have been investigated and a phase diagram has been constructed.

1. Introduction

Room temperature molten salts (RTMSs), sometimes recently called room temperature ionic liquids, have received attention for their excellent characteristics from the viewpoint of electrochemical and synthetic applications [1-5]. In 1999, we developed new RTMS, 1-ethyl-3-methylimidazolium fluorohydrogenates, $EMIm(HF)_{2.3}F$, having a high ionic conductivity of 10^2 mS cm^{-1} at 298 K [6]. Since then, we have reported some fundamental studies on physical and chemical properties of 1-alkyl-3-methylimidazolium fluorohydrogenates $(RMIm(HF)_{2.3}Fs)$ [7,8], electrochemical [9-11] and synthetic [12-15] applications.

$EMIm(HF)_{2.3}F$ and other dialkylimidazolium fluorohydrogenates possess negligibly small dissociation pressure at room temperature which contrasts to alkali metal fluorohydrogenates that liberate HF more or less under reduced pressure. However, fluorohydrogenate anions slightly liberate HF at elevated temperatures and evacuation of the salt gives HF-deficient $EMIm(HF)_nFs$ ($n < 2.3$). Naturally, these HF-deficient salts are thermally stable at elevated temperature compared to $EMIm(HF)_{2.3}F$, which would expand the application field of these salts.

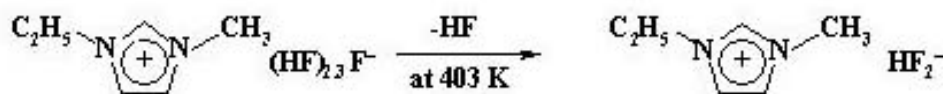The reaction of EMImCl with a stoichiometric amount of HF is not a suitable method for preparation of $EMIm(HF)_nFs$ with n < 2.3, giving only a mixture of EMImCl and $EMIm(HF)_nF$. $EMImHF_2$

2

(EMIm(HF)$_{1.0}$F) prepared by the elimination of HF from EMIm(HF)$_{2.3}$F at 403 K is a solid salt of EMIm cation and HF$_2^-$ at room temperature [16]. The reaction of EMImHF$_2$ with HF gives EMIm(HF)$_n$F which is a technically superior method to control the n value of EMIm(HF)$_n$F compared to the thermal decomposition method. Fluorohydrogenate anions, (HF)$_n$F$^-$, characterized in the previous studies for alkaline metal [17-25] and alkylammonium fluoride-HF [26] systems are also expected to be present in EMImF-HF system. Figure 1 shows the structures of fluorohydrogenate anions, HF$_2^-$, (HF)$_2$F$^-$ and (HF)$_3$F$^-$. Computational studies on the structures of these anions are available in the literature [27-29]. The fractions of anions such as HF$_2^-$, (HF)$_2$F$^-$ and (HF)$_3$F$^-$ anions in the salt are expected to change with the change of n, as is case for other systems.

In this paper, the anionic species present in the EMIm(HF)$_n$Fs are identified by IR spectroscopy and the effects of their fractions on the thermal and electrochemical properties have been studied. A phase diagram of EMIm(HF)$_n$Fs (n) has been constructed in the range of n = 1.0~2.6.

2. Experimental

2-1 Synthesis.

EMIm(HF)$_{2.3}$F was prepared according to the method previously reported [7,8]. Synthesis of EMImHF$_2$ was made by elimination of HF from EMIm(HF)$_{2.3}$F at 403 K. HF was evacuated by a rotary pump through a chemical trap for one day and then directly through a cold trap for three days [16].

Scheme 1

3

Synthesis of EMIm(HF)$_n$F was made by the stoichiometric reaction of EMImHF$_2$ with HF.
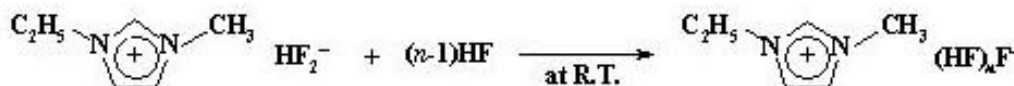

Scheme 2

2-2   Analysis.

IR spectra of EMIm(HF)$_n$F were obtained by an FTIR spectrometer, BIO-RAD Laboratories, FTS165. EMIm(HF)$_n$F was sandwiched between a pair of AgCl crystal windows in an airtight cell. Thermal analysis of the molten salts was performed with the aid of a Shimadzu DSC-60 in N$_2$ atmosphere at the cooling and heating rates of 10 K· min^{-1}. Electrochemical windows of EMIm(HF)$_n$F were determined by cyclic voltammetry and compared using ferrocene / ferricenium cation redox potential as a standard potential [30]. Electrochemical measurement was performed with the aid of a Hokuto Denko HZ-3000 electrochemical measurement system. The working electrode was made of a glassy carbon disk, and counter and quasi-reference electrodes were made of platinum wire. Molten salts in which the reference electrode was immersed were separated by a polyflon filter (Advantec Toyo Kaisha, Ltd., PF020) from the compartment where the working and counter electrodes were placed, so that the reference electrode was not affected by the reactions at the working and counter electrodes. Conductivity was measured by an impedance technique using a calibrated cell with platinum disk electrodes. Unlike the case of EMIm(HF)$_{2.3}$F, HF deficient salts are hygroscopic. Sample handling and the measurements were performed in an airtight system.

3. Results and discussion

3-1 IR spectra.

Figure 2 shows the IR spectra of $EMIm(HF)_nFs$ (n = 1.3~2.3) in which the peak positions of HF_2^- found for KHF_2 [18,20,21,25] are marked by dashed lines. Although the changes in the spectra are not clear due to the overlap of the peaks of the cation, the intensity of the peak at 1250 cm^{-1} for example decreases as the n increases, and the peak is completely missing in the spectrum of $EMIm(HF)_{2.3}F$. It is concluded that the fraction of HF_2^- anion in the salt decreases with the increase of n. Figure 3 shows again the same IR spectra in which the peak positions of $(HF)_2F^-$ and $(HF)_3F^-$ found for $K^+(HF)_2F^-$ [22,24,25], $K^+(HF)_3F^-$ [24,25], respectively, are marked with dashed lines. The peak positions of these anions found for other salts such as alkylammonium fluorohydrogenates are not significantly changed [26]. It is suggested that the dominant anions in $EMIm(HF)_nFs$ (n = 1.0~2.0) are HF_2^- and $(HF)_2F^-$. Peaks ascribed to $(HF)_3F^-$ are not detected in this composition range suggesting that the fraction of $(HF)_3F^-$ is negligibly small. In the case of $EMIm(HF)_{2.3}F$ the peaks ascribed to $(HF)_3F^-$ are rather faint but observable. Figure 4 shows a schematic diagram of the changes in the fractions of $(HF)_nF^-$ with n based on the simple mixed salt model. The anionic species in $EMImHF_2$ ($EMIm(HF)_{1.0}F$) is HF_2^- as proved by x-ray crystallography [16]. The anions existing in $EMIm(HF)_nF$ (n = 1.0~2.0) are HF_2^- and $(HF)_2F^-$, and that in $EMIm(HF)_2F$ is $(HF)_2F^-$, and $(HF)_2F^-$ and $(HF)_3F^-$ are the anionic species in $EMIm(HF)_nF$ (n = 2.0~3.0). This distribution of the anionic species can be explained as a result of sequential dissociation of fluorohydrogenate anions (eq. 1).

$$(HF)_{n+1}F^- \rightleftharpoons (HF)_nF^- + HF \qquad\qquad (1)$$
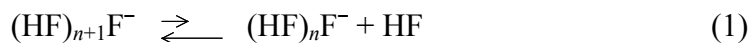
Thus the acidity of EMImF-HF system can be controlled by changing the number of HF molecules involved in the anions $(HF)_nF^-$, as in the case of the $EMImCl-AlCl_3$ system [31].

3-2 Thermal property.

Figure 5 shows a DSC thermogram of EMIm(HF)$_{2.3}$F. EMIm(HF)$_{2.3}$F is supercooled to show a glass-like behavior below the melting point. In the heating process, the supercooled salt is crystallized at 186 K and then melts again at 208 K. EMIm(HF)$_n$Fs (n = 1.8~2.3) show DSC thermograms similar to that of EMIm(HF)$_{2.3}$F. EMIm(HF)$_n$Fs (n = 2.4~2.6) do not exhibit the peaks of glass transition on the cooling curve, indicating that this transition is below 140 K, the lower limit of the measurable temperature of the apparatus. Figure 6 shows a DSC thermogram of EMIm(HF)$_{1.5}$F. In the cooling process, a solid precipitates from the melt at 263 K and the remaining liquid is frozen at 223 K. EMIm(HF)$_n$Fs (n = 1.0~1.6) show DSC thermograms similar to that of EMIm(HF)$_{1.5}$F. Figure 7 shows a DSC thermogram of EMIm(HF)$_{1.1}$F that melts at 308 K. Another small peak found at 251 K is a phase transition from solid solution to solid liquid system. Table 1 shows the melting points and glass transition temperatures of EMIm(HF)$_n$Fs (n = 1.0~2.6). EMIm(HF)$_n$Fs (n = 1.3~1.7) show two peaks of melting, the precipitations of two different solids being observed. EMIm(HF)$_n$Fs (n = 1.8~2.6) exhibit a peak of melting and a peak of glass transition. In the heating process, solid precipitation in the liquid is observed below 220 K for EMIm(HF)$_n$Fs (n = 1.8~2.3).

EMIm(HF)$_n$Fs with smaller n possess lower dissociation pressures at elevated temperature. The dissociation pressure of EMIm(HF)$_{1.7}$F is lower than 1 Pa even at 343 K.

3-3 Construction of a phase diagram of EMImF-HF system.

Figure 8 shows the plots of the melting points and glass transition temperatures of EMIm(HF)$_n$Fs (n = 1.0~2.6). EMIm(HF)$_n$Fs (n = 1.0~1.7) show a solid-liquid two phase system at 220 to 324 K, and EMIm(HF)$_n$Fs (n = 1.0~1.5) show two solid phases below 220 K. EMIm(HF)$_n$Fs (n> 1.7) show one solid precipitation in the cooling process. The melting points of EMIm(HF)$_n$Fs (n = 1.7~2.0) appear at ~ 220 K and sharply fall as n becomes close to 2.0. The melting points of EMIm(HF)$_n$Fs (n = 2.0~2.6) appear at ~ 220 K and gradually fall as n increases.

6

Five compounds, KHF_2, $K(HF)_2F$, $K(HF)_{2.5}F$, $K(HF)_3F$ and $K(HF)_4F$ have been found in the phase diagram of the KF-HF system [17]. Seven compounds appear in the phase diagram of the RbF-HF system [23]; $RbHF_2$, $Rb(HF)_{1.5}F$, $Rb(HF)_2F$, $Rb(HF)_{2.5}F$, $Rb(HF)_3F$, $Rb(HF)_4F$ and $Rb(HF)_7F$. In the case of CsF-HF system, four compounds have been reported [19]; $CsHF_2$, $Cs(HF)_2F$, $Cs(HF)_3F$ and $Cs(HF)_6F$. As in the alkaline metal fluoride-HF systems in which complex salts of $(HF)_nF^-$ are formed, $EMIm(HF)_nFs$ (n = 1~3) are also expected to give compounds such as $EMImHF_2$, $EMIm(HF)_{1.5}F$, $EMIm(HF)_2F$, $EMIm(HF)_{2.5}F$ and $EMIm(HF)_3F$. Figure 9 shows the phase diagram of $EMIm(HF)_nFs$ (n = 1.0~2.6) in the present study constructed based on the results shown in Figure 8 and the phase rule. $EMIm(HF)_nFs$ (n = 1.3~1.7) give the solidus line at 220 K. $EMIm(HF)_nFs$ (n = 1.0~1.7) between 220 K and room temperature give a solid-liquid phase, and $EMImHF_2$ does not show a phase transition at 220 K, thus two solid phases are considered to appear below 220 K. $EMIm(HF)_nFs$ (n < 1.1) are solid solutions of $EMImHF_2$ containing small amounts of $EMIm(HF)_{1.5}F$. $EMIm(HF)_nFs$ (n = 1.1~1.7) give $EMImHF_2$ solid solution and a liquid phase between ~220 K and room temperature. $EMIm(HF)_nFs$ (n = 1.0~1.5) give two solid phases, $EMImHF_2$ solid solution and presumably $EMIm(HF)_{1.5}F$, below 220 K, and in the range of n = 1.7~2.0, $EMIm(HF)_{1.5}F$ and a liquid phase appear below the melting point of $EMIm(HF)_{1.5}F$. $EMIm(HF)_nFs$ (n = 2.0~2.6) give solid $EMIm(HF)_2F$ and a liquid phase. Thus the phase diagram suggests the existence of the compounds $EMIm(HF)_{1.5}F$ and $EMIm(HF)_2F$, although the structural characterization has not been completed due to the difficulty of single crystal preparation and manipulation of these compounds in viscous liquids at such low temperatures.

For the region of n < 1.0, all efforts to isolate $EMIm^+F^-$ as a solid compound by ion exchange in solvents other than HF were unsuccessful. The basicity of naked fluoride ion is too strong to form an ionic salt without decomposing the EMIm cation under ambient conditions. It can be present only in solution where fluoride ion is solvated by solvent molecules and the basicity of fluoride ion is attenuated [32]. Hydrated 1-butyl-3-methylimidazolium fluoride, $BMImF \cdot H_2O$ has been isolated as a solid compound by hydrolysis of hexafluorophosphate [33].

3-4   Electrochemical windows.

Figure 10 shows the cyclic voltammograms, and Table 2 shows the electrochemical windows of EMIm(HF)$_n$Fs. Note that the anode limit potential of EMIm(HF)$_{1.6}$F is ~1.6 V vs Pt Q.R.E. like that of the other salts on the figure although the first anodic peak near the anode limit is small and does not exceed 0.5 mAcm^{-1} at which the sweep is routinely reversed. The electrochemical windows are constant at ~ 3 V regardless of the n value except that of EMIm(HF)$_{1.6}$F, which is slightly larger (3.43 V). As has been discussed in the previous work [7], the cathode limit reaction probably includes both the reduction of cation and anion, the latter being accompanied by H$_2$ evolution. The reaction at the anode limit is probably the decomposition accompanied by fluorination of the cation. Although the electrochemical windows do not show clear dependence on n, the difference mostly arises from the difference of the cathode limit and similar anode limits are observed regardless of n (1.6 to 1.7 V).

3-5   Conductivity.

Figure 11 shows the temperature dependence of the conductivity of EMImHF$_2$ and EMIm(HF)$_{2.3}$F. Figure 12 shows the conductivities of EMIm(HF)$_n$Fs at 298 K. The conductivity of EMIm(HF)$_n$Fs is almost proportionally increased with the increase of n in this composition range. This is explained by the decrease of electrostatic interaction between the imidazolium cation and anion of which the basicity decreases with the increase of HF attached to the fluoride ion. The decrease of the electrostatic interaction between the cation and anion decreases the association of the ions. As a result, the ionic conductivity is increased as the viscosity decreases. Although the viscosity measurement of small amount of hygroscopic salt in an airtight system is technically difficult for us now, the decrease of viscosity of the salt sealed in a sealed container with the increase of n was easily observed by eye.

The conductivity of EMIm(HF)$_{2.3}$F at room temperature decreased with the decrease of the n value and was halved for EMIm(HF)$_{1.3}$F. However, this would not be a significant disadvantage of these HF-deficient salts since their practical applications would be for use at elevated temperatures where the

conductivity is enhanced. As found in Fig. 11, even $EMImHF_2$ ($n = 1$) exhibits the same conductivity at 363 K as that of $EMIm(HF)_{2.3}F$ at room temperature.

4.   Conclusion

The effects of the structures of anions on the thermal and electrochemical properties of $EMIm(HF)_nFs$ have been investigated. $EMIm(HF)_nFs$ are composed of EMIm cation and fluorohydrogenate anions, $(HF)_nF^-$, of which the fractions change with the change of n. A phase diagram of $EMIm(HF)_nFs$ ($n = 1.0\sim2.6$) has been constructed which suggests the presence of the stoichiometric compounds, $EMIm(HF)_{1.5}F$ and $EMIm(HF)_2F$. $EMIm(HF)_{1.8}F$ possesses a wide liquid temperature range due to its high thermal stability at elevated temperatures. The electrochemical windows of $EMIm(HF)_nFs$ ($n = 1.0\sim2.6$) fall in the range of 2.9-3.4 V without showing clear dependence on n. The conductivity of $EMIm(HF)_nFs$ ($n = 1.0\sim2.6$) increases with the increase of n.

Figure Captions.

Figure 1 Molecular structures of HF_2^-, $(HF)_2F^-$ and $(HF)_3F^-$.

Figure 2 IR spectra of $EMIm(HF)_nF$. The dashed lines (---) are the peak positions of HF_2^- found in the solid state. (a) EMImCl, (b) $EMIm(HF)_{1.3}F$, (c) $EMIm(HF)_{1.5}F$, (d) $EMIm(HF)_{1.6}F$, (e) $EMIm(HF)_{1.8}F$, (f) $EMIm(HF)_{2.3}F$.

Figure 3 IR spectra of $EMIm(HF)_nF$. The dashed lines (---) and dotted lines (⋯) are the peak positions of $(HF)_2F^-$ and $(HF)_3F^-$ found in the solid state. (a) EMImCl, (b) $EMIm(HF)_{1.3}F$, (c) $EMIm(HF)_{1.5}F$, (d) $EMIm(HF)_{1.6}F$, (e) $EMIm(HF)_{1.8}F$, (f) $EMIm(HF)_{2.3}F$.

Figure 4 Schematic diagram of the anion fraction of $(HF)_nF^-$ in $EMIm(HF)_nF$.

Figure 5 DSC thermogram of $EMIm(HF)_{2.3}F$. Scan rate: 10 K min^{-1}.

Figure 6 DSC thermogram of $EMIm(HF)_{1.5}F$. Scan rate: 10 K min^{-1}.

Figure 7 DSC thermogram of $EMIm(HF)_{1.1}F$. Scan rate: 10 K min^{-1}.

Figure 8 Plots of the melting point and glass transition temperature of $EMIm(HF)_nF$.

Figure 9 Phase diagram of $EMIm(HF)_nF$ ($n = 1.0~2.6$)

Figure 10 Cyclic voltammogram of a glassy carbon disk electrode in $EMIm(HF)_nF$. W.E.: G.C. disk, C.E.: Pt plate, Q.R.E.: Pt wire, scan rate: 10 mV s^{-1}.

Figure 11 Temperature dependence of conductivities of $EMImHF_2$ and $EMIm(HF)_{2.3}F$.

Figure 12 Conductivities of $EMIm(HF)_nF$ at 298 K.

10

Scheme Titles.

Scheme 1 Synthesis of EMImHF$_2$.

Scheme 2 Synthesis of EMIm(HF)$_n$F (n = 1.0~2.6)

Tables

Table 1 Melting points and glass transition temperatures of EMIm(HF)$_n$Fs (n =1.0~2.6)

n	Melting point / K	Glass transition temperature
1.00	324	-
1.12	251, 308	-
1.34	219, 281	-
1.51	217, 273	-
1.67	221, 242	-
1.79	223	152
1.86	221	149
1.92	217	147
1.95	212	148
2.01	223	150
2.19	212	146
2.24	215	147
2.28	208	148
2.33	214	145
2.35	212	145
2.45	205	< 140
2.57	202	< 140

Table 2 Electrochemical windows of $EMIm(HF)_nFs$

$EMIm(HF)_nF$	Electrochemical windows / V
$EMImHF_2$	3.02 (353 K)
$EMIm(HF)_{1.3}F$	3.18 (298 K)
$EMIm(HF)_{1.6}F$	3.43 (298 K)
$EMIm(HF)_{1.8}F$	2.88 (298 K)
$EMIm(HF)_{2.3}F$	2.95 (298 K)

References

(1) Seddon, K. R. *J. Chem. Technol. Biotechnol.*, **1997**, *68*, 351.

(2) Welton, T. *Chem. Rev.*, **1999**, *99*, 2071.

(3) Wasserscheid, P.; Kein, W. *Angew. Chem. Int. Ed.*, **2000**, *39*, 3772.

(4) Hagiwara, R.; Ito, Y. *J. Fluorine Chem.*, **2000**, *105*, 221.

(5) Hagiwara, R. *Electrochemistry*, **2002**, *70*, 130.

(6) Hagiwara, R.; Hirashige, T.; Tsuda, T.; Ito, Y. *J. Fluor. Chem.*, **1999**, *99*, 1.

(7) Hagiwara, R.; Hirashige, T.; Tsuda, T.; Ito, Y. *J. Electrochem. Soc.*, **2002**, *149*, D1.

(8) Hagiwara, R.; Matsumoto, K.; Nakamori, Y.; Tsuda, T.; Ito, Y.; Matsumoto, H.; Momota, K. *J. Electrochem. Soc.,* **2003***, 150*, D195.

(9) Matsumoto, H.; Matsuda, T.; Tsuda, T.; Hagiwara, R.; Ito, Y. Miyazaki, Y. *Chem. Lett.*, **2001**, *26.*

(10) Tsuda, T.; Nohira, T.; Nakamori, Y.; Matsumoto, K.; Hagiwara, R.; Ito, Y. *Solid St. Ionics*, **2002**, *149*, 295.

(11) Ue, M.; Takeda, M.; Toriumi, A.; Kominato, A.; Hagiwara, R.; Ito, Y. *J. Electrochem. Soc.*, **2003**, *150*, A499.

(12) Matsumoto, K.; Hagiwara, R.; Ito, Y. *J. Fluor. Chem.*, **2002**, *115*, 133.

(13) Matsumoto, K.; Hagiwara, R.; Yoshida, R.; Ito, Y.; Mazej, Z.; Benkič, P.; Žemva, B.; Tamada, O.; Yoshino, H.; Matsubara, S. *Dalton Trans*., **2004**, 144.

(14) Yoshino, H.; Matsubara, S.; Oshima, K.; Matsumoto, K.; Hagiwara, R.; Ito, Y. *J. Fluor. Chem.*, **2004**, *125*, 455.

(15) Yoshino, H.; Nomura, K.; Matsubara, S.; Oshima, K.; Matsumoto, K.; Hagiwara, R.; Ito, *J. Fluor. Chem*., **2004**, in press.

(16) Matsumoto, K.; Tsuda, T.; Hagiwara, R.; Ito Y.; Tamada, O. *Solid State Sciences*, **2002**, *4*, 23.

(17) Cady, G.H. *J. Am. Chem. Soc.* **1934**, *56*, 1431.

(18) Ketelaar, J.A.A. *J. Chem. Phys.* **1941**, *9*, 775.

(19) Winsor, R.V.; Cady, G.H. *J. Am. Chem. Soc.* **1948**, *70*, 1500.

(20) Ketelaar, J.A.A.; Vedder, W. *J. Chem. Phys.* **1951**, *19*, 654.

(21) Coté, G.L.; Thompson, H.W. *Proc. Roy. Soc.* **1952**, *210A*, 206.

(22) Ažman, A.; Ocvirk, A.; Hadži, D.; Giguére P.; Schneider, M. *Can. J. Chem.*, **1967**, *45*, 1347.

(23) Boinon, B.; Marchand, A. *J. Therm. Anal.*, **1976**, *10*, 411.

(24) Harmon, K.M.; Gennick, I. *J. Mol. Struct.*, **1977**, *38*, 97.

(25) Omori, H. *Master's thesis in Kyoto University*, **1996**.

(26) Gennick, I.; Harmon, K. M.; Potvin, M. M. *Inorg. Chem.*, **1977**, *16*, 2033.

(27) Clark, J. H.; Emsley, J.; Jones, D. J.; Overrill, R. E. *J. Chem. Soc., Dalton Trans.*, **1981**, 1219.

(28) Chandler, W. D.; Johnson, K. E.; Campbell, J. L. E. *Inorg. Chem.*, **1995**, *34*, 4943.

(29) Rosenvinge, T. v.; Parrinello, M.; Klein, M. L. *J. Chem. Phys.*, **1997**, *107*, 8013.

(30) Gritzner, G.; Kuta, J. *Pure Appl. Chem.* **1984**, *56*, 461.

(31) Fannin, A.A. Jr.; Floreani, D.A.; King, L.A.; Landers, J.S.; Piersma, B.J.; Stech, D.J.; Vaughn, R.L.; Wilkes, J.S.; Williams, J. L. *J. Phys. Chem.*, **1984**, *88*, 2614.

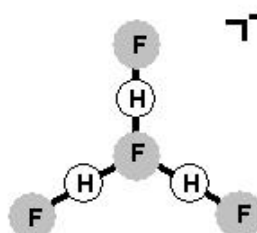(32) Ue, M.; Takeda, M.; Takahashi, T.; Takehara, M. *Electrochem. Sol. St. Lett.*, **2002**, *5*, A119.

(33) Swatloski, R.P.; Holbrey, J.D.; Rogers, R.D. *Green Chem.*, **2003**, *5*, 361.

HF_2^- (bifluoride ion, $D_{\infty h}$)
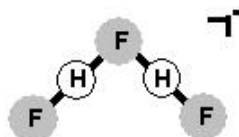
$(HF)_2F^-$ (μ-fluoro-bis(fluolohydrogenate) ion, C_{2v})

$(HF)_3F^-$ (μ_3-fluoro-tris(fluolohydrogenate) ion, D_{3h})

Fig. 1   *Hagiwara et al.*

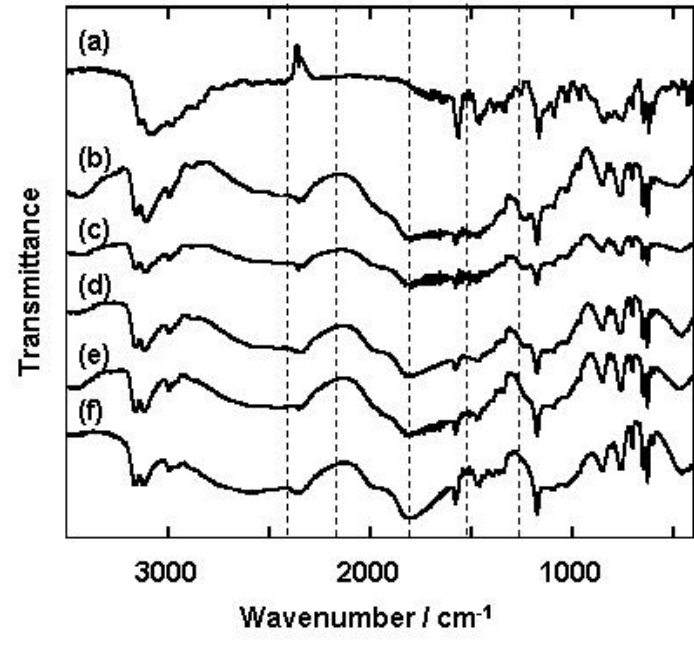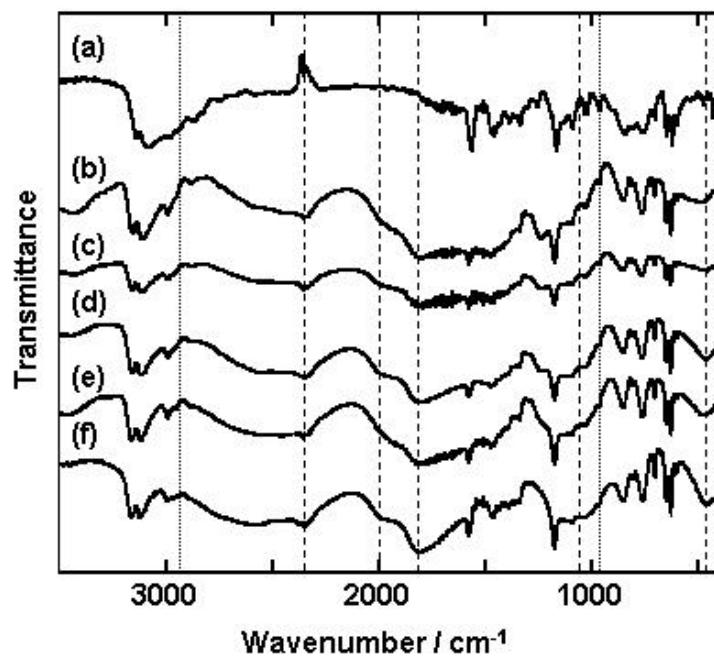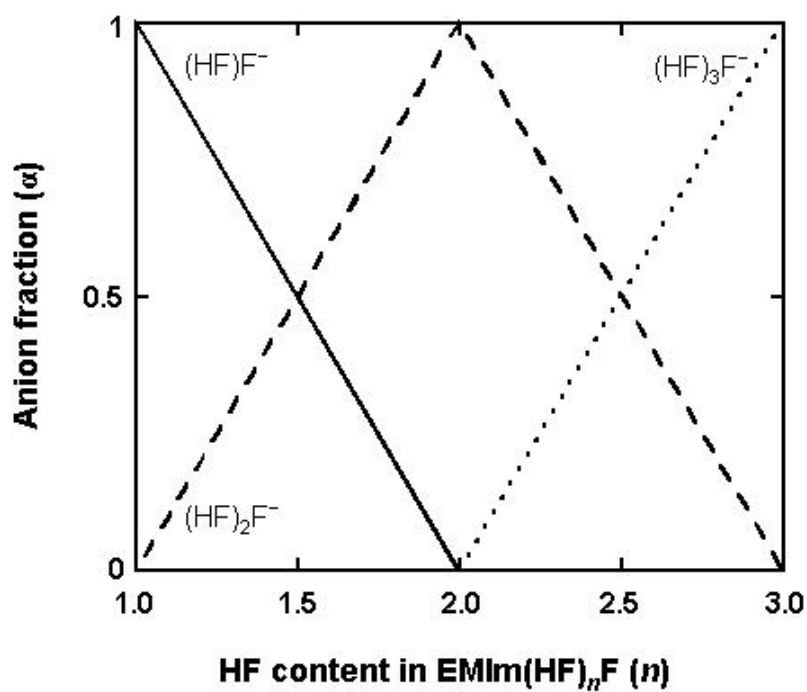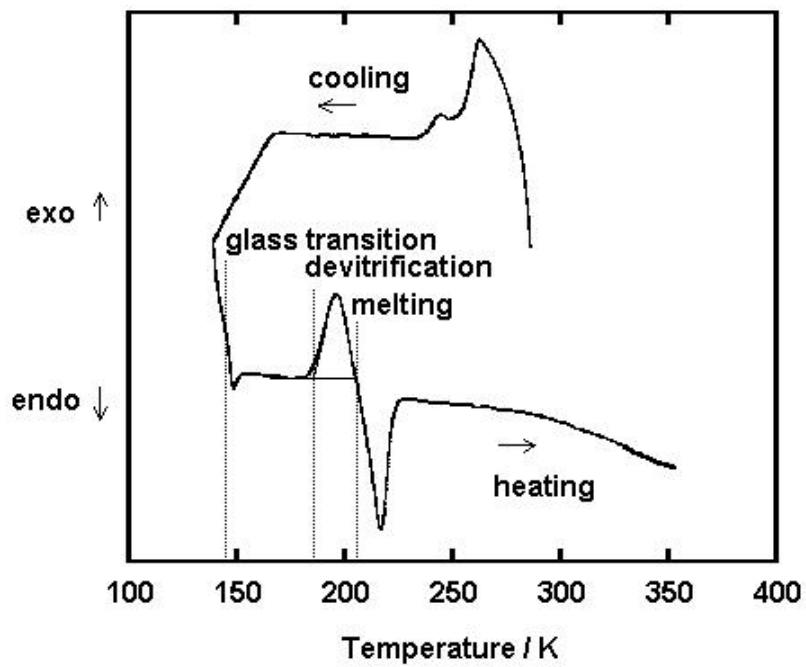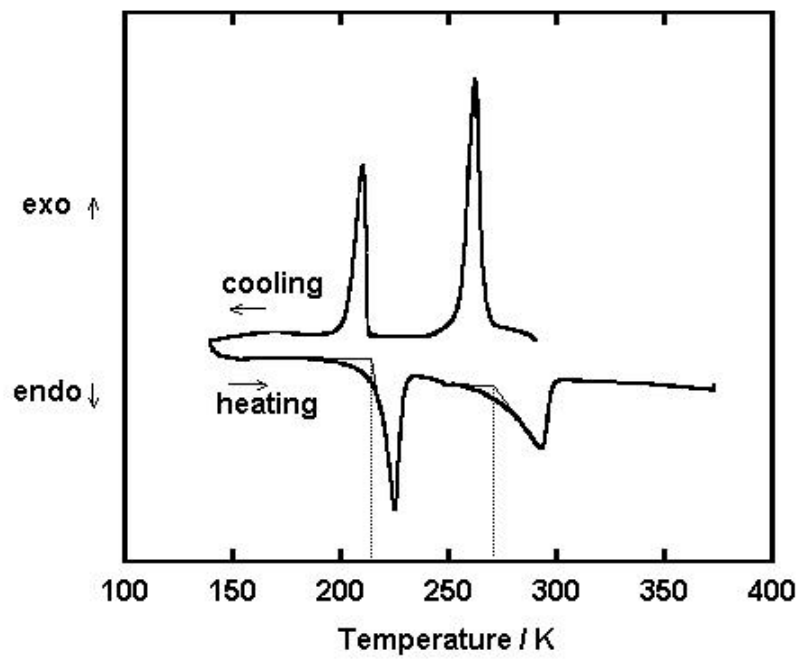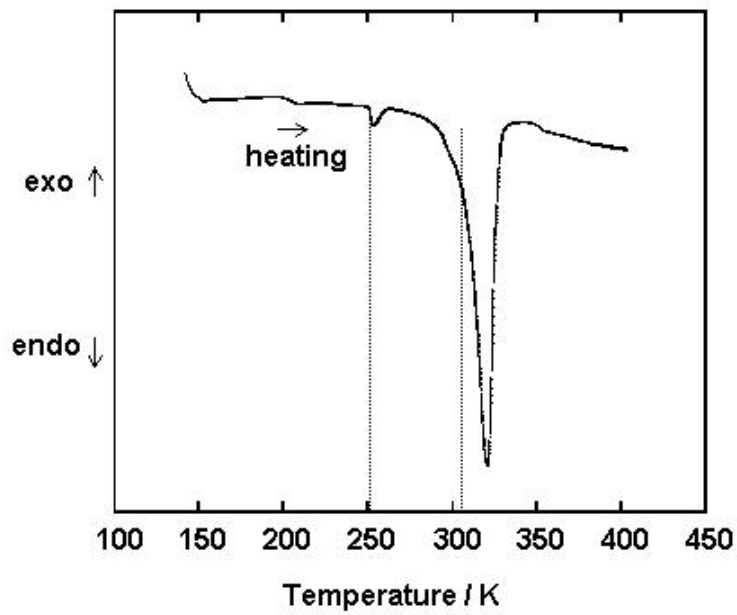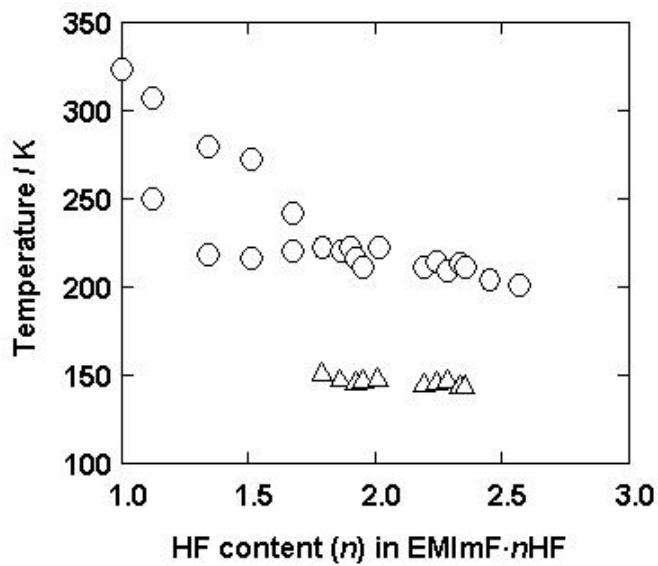Fig. 2   *Hagiwara et al.*

Fig. 3   *Hagiwara et al.*

京都大学

$$\alpha_{(HF)_nF^-} = \frac{C_{(HF)_nF^-}}{C_{(HF)F^-} + C_{(HF)_3F^-} + C_{(HF)_2F^-}}$$

Fig. 4   *Hagiwara et al.*

Fig. 5   *Hagiwara et al.*

Fig. 6   *Hagiwara et al.*

exo ↑

endo ↓

heating

Temperature / K

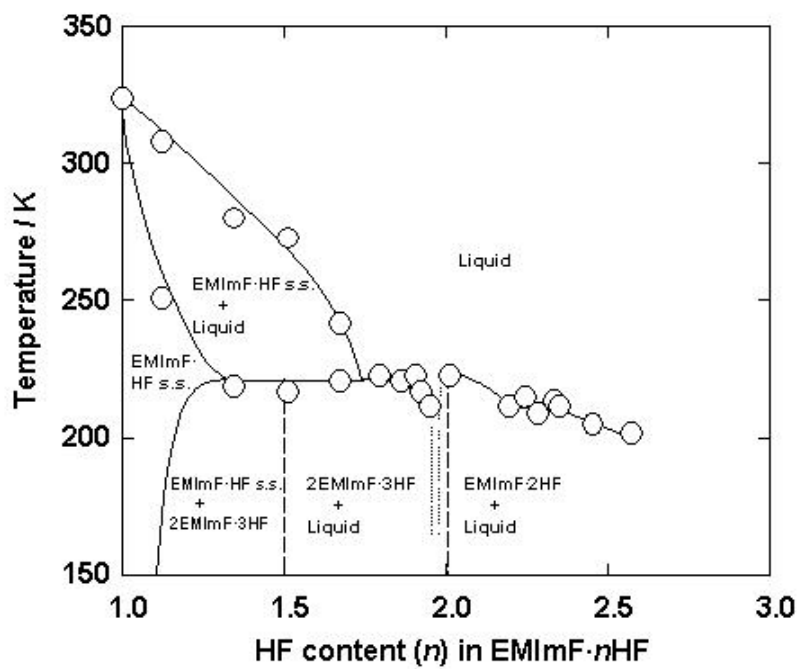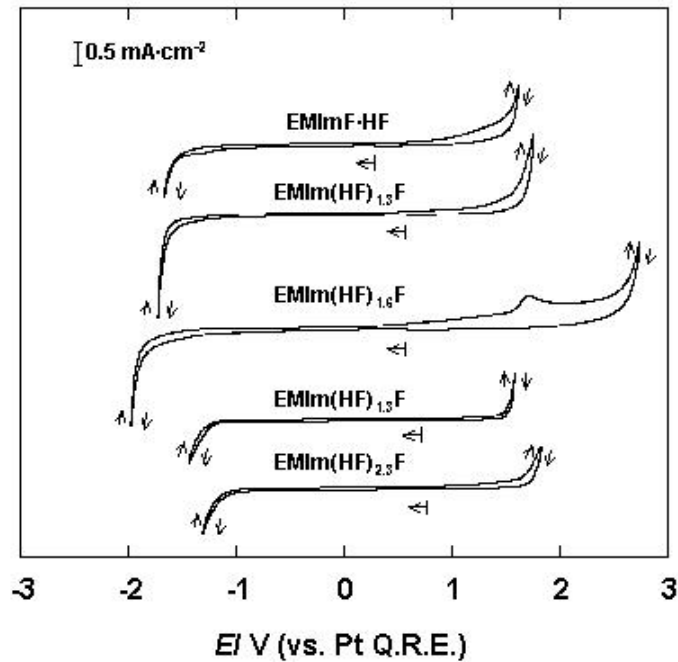Fig. 7   Hagiwara et al.

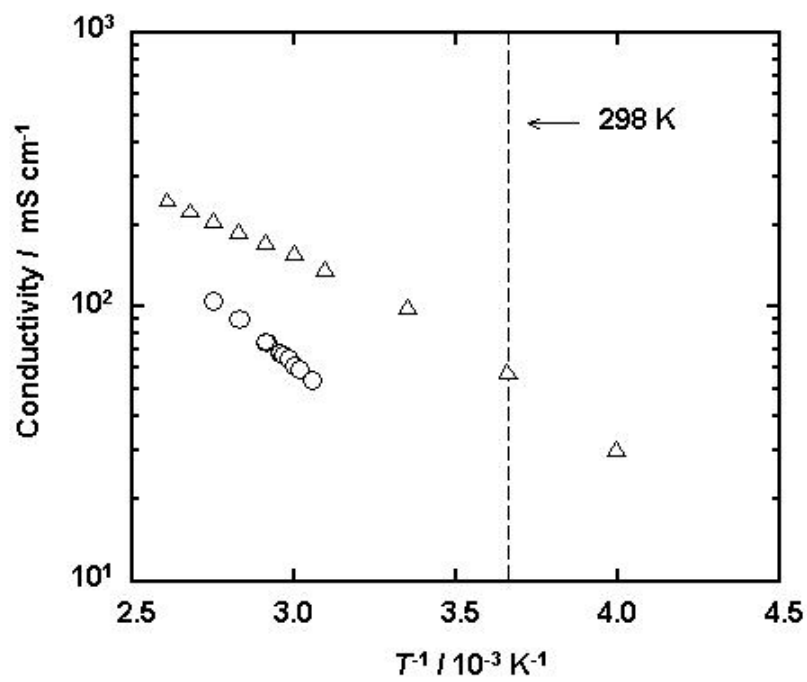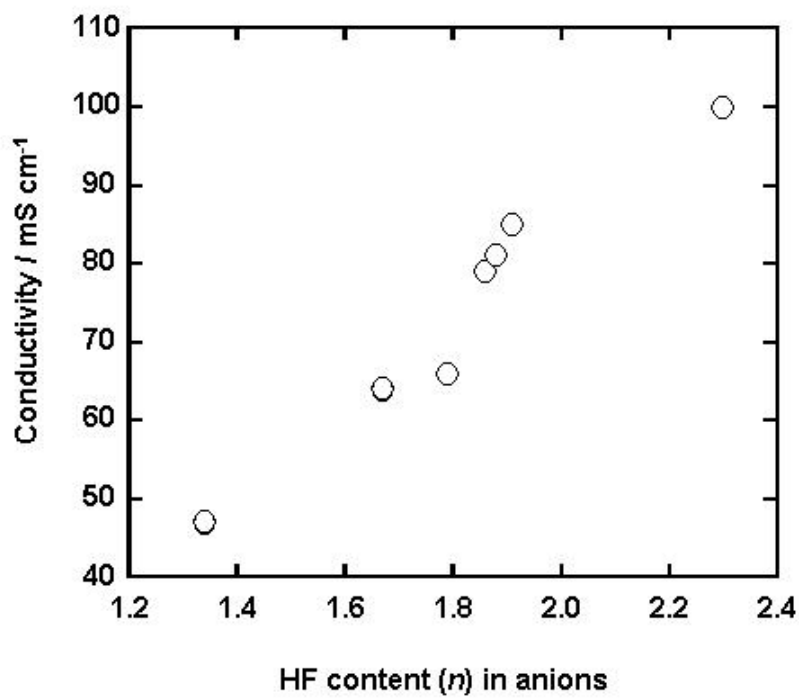Fig. 8   *Hagiwara et al.*

Fig. 9   *Hagiwara et al.*

Fig. 10   *Hagiwara et al.*

Fig. 11   *Hagiwara et al.*

Fig. 12   *Hagiwara et al.*